www.czasopisma.pan.pl PAN POLSKA AKADEMIA NAUK www.journals.pan.pl

Arch. Metall. Mater. **63** (2018), 1, 481-490

DOI: 10.24425/118965

H. BĄKOWSKI*#

WEAR MECHANISM OF SPHEROIDAL CAST IRON PISTON RING-ALUMINUM MATRIX COMPOSITE CYLINDER LINER CONTACT

The paper presents the results of research on the impact of stereological characteristics of microstructure of graphite in nodular GJS-400 cast iron and Al_2O_3 fibers in the composite AC-47000 + 10% Al_2O_3F on the mechanism of wear in a cast iron piston ring – composite cylinder liner contact in a combustion engine.

To elucidate the mechanisms of wear in the tested contact was used Finite Element Method (FEM). On the basis of quantitative metallographic examination of test materials were determined stereological parameters of their structures. It was necessary for the implementation of the 3D model that reflects the actual structure with particular focus on the different phases in order to determine the distribution of stresses and strains. The determination Strains of the local stresses value of allowed the prediction of wear initiating places. Formation of stereological parameters of cast iron in the technological process allows a prediction of values and distributions of the stresses/strains and thus reduce wear and extend durability of the analyzed contact.

Keywords: cast iron, spheroidal graphite, wear mechanism, stereological parameters

1. Introduction

Spheroidal cast iron is a gray cast iron with graphite in the form of spheres. This cast iron has a much higher ultimate strength (Su of 400 to 900 MPa) and improved tribological properties than cast iron with lamellar graphite (Su of 100 to 400 MPa). In the automotive industry is widely used due to the favorable ratio of property to the cost of production [1]. Cast iron is used for the production of crankshafts and camshafts, rockers, cylinder liners, pistons and piston rings [2]. So extensive use of nodular cast iron is dictated greater wear resistance compared to lamellar gray cast iron [3]. In order to elucidate the mechanisms of wear and prediction of the properties of cast iron are made tribological tests using laboratory testers, the results of which are confirmed in studies of real objects. Increasingly, because of the costs are used Finite Element Method. It allows determining the distribution and the values of stresses and strains in the surface layer of cast iron. The use of the FEM to determine the stresses in the material at the stage of preparation of such casting solidifications [4,5] may be useful in elucidating the mechanisms of wear, and a cost-effective manufacture of machine parts [6].

Stereological features of graphite precipitates in cast iron have a significant effect on its mechanical properties and wear mechanism [7,8]. Analysis of deformation of the matrix of cast iron in the vicinity of spheroidal graphite precipitates made using FEM has shown that they lead to subsurface cracks in cast iron. In [9,10], can be found information about the possibilities of using FEM to predict the direction of crack propagation.

Modelling using FEM to determine the critical value stresses/strains and estimated durability it has a high conformability of results of numerical calculations with experimental results [11]. In [12], the authors point out that the materials that have heterogeneous properties in the entire volume the maximum stresses does not always coincide with the maximum strains. This is extremely important from the point of view of fatigue life prediction and machine parts uptime, made of a material with a heterogeneous microstructure such as nodular cast iron.

In the earlier works of the author [13,14] was used FEM for modeling of microstructure of cast iron with lamellar graphite. Calculated distributions of stresses and strains in the elements of cast iron structure allowed the elucidation of the mechanisms of cast iron piston ring-composite cylinder liner contact's wear. To build the model on a structure level were used stereological characteristics parameters of structural components, i.e. proper and relative surface area, the average distance between precipitates, the volume fraction, diameter and the shape indicator. These features have an significant effect on the mechanical properties of materials and tribological properties of a contact. Surface fraction of graphite determines the lubricating properties of contact, while the number of graphite precipitates per unit area can determine the dispersion of precipitates. In addition, the average distance between precipitates allows to determine how often fibers Al_2O_3 will be in contact with the cast iron matrix (pearlite).

* SILESIAN UNIVERSITY OF TECHNOLOGY DEPARTMENT OF AUTOMOTIVE VEHICLES SERVICE FACULTY OF TRANSPORT ,8 KRASIŃSKIEGO STR., 40-019 KATOWICE, POLAND

Corresponding author: henryk.bakowski@polsl.pl

Flake graphite precipitates in gray cast iron are being used worn slowly than the spheroidal one in nodular cast iron because of the large development of their surface [15]. In nodular cast iron near of graphite precipitates is a decarburized zone in which the graphite content is lower. Therefore, after spalling graphite precipitates arises the area of pearlitic matrix with a deficiency of graphite acting as a solid lubricant, which worsens the tribological properties. This article is dedicated to explaining the differences in wear mechanisms of cast iron with flake graphite and spheroidal cast iron sliding against the composite reinforced with ceramic fibers.

For the analysis of each phase was used the program for quantitative metallographic analysis which allows determining the representative value of the microstructure. At the used measurement method the relative error of assessment of the volume fraction of the phases and structural components does not exceed 5%. Stereological properties allow mathematically and objectively present the distribution, dimension and shape of individual phases in the structure, which allows to determine the distribution of local stresses and strains facilitating durability prediction under consideration of friction node. All phases of the structure take an active part in the process of friction and have a significant impact on the mechanism and intensity of wear. The result of the analysis is a set of numbers that describe the characteristics of the selected structure. Only in quantitative metallography – specified by number and unit of measurement – can be found close relationships between structure and properties. For computer image analysis were used only the geometrical characteristics of the analyzed objects that have a direct impact on the properties of the material. Used indicators allow illustrating the shape of the particles in question.

2. Experimental details

The study conducted at the Department of Transport of Silesian University of Technology were investigated the contact made of nodular cast iron (GJS 400) piston ring-cylinder liner made of composite with AC 47000 alloy matrix reinforced by the addition of 10% of alumina fibers. The study was performed in two stages. In the first stage was set stereological features of tested materials, the model of contact and calculations of the distribution of stresses and strains in the contact zones. In the second stage performed: tribological tests, microscopic and profilometry surface examination after friction and wear products filtered from the oil by chemical means (isopropanol) and membrane drains in accordance with ISO 16232.

Measuring the stereological characteristics of the tested materials were made according to the requirements of ASTM E112 and ASTM A247 on more than 1000 objects on polished cros-sections using the program for quantitative metallographic analysis which allows to determine the histogram of average size of graphite precipitates distribution. This enabled the creation of a geometric model of the microstructure, which reflects the actual dimensions and distribution of the various phases in the alloy. Simulation studies were carried out using the Finite Element Method. Displayed geometrical models were made on the basis of metallographic analysis taking into account the dimensions and shape of the various phases in the structure. Calculations were carried out with regard to the actual operational conditions prevailing in the contact of the piston gas ring with the cylinder liner in internal combustion engine, i.e. the pressure of 3 MPa and a coefficient of friction of 0.1. Calculations were made for the two extreme positions of the fibers in the composite (Fig. 6), at which the movement of the castiron ring held along the fibers of Al_2O_3 (V_1) and transverse to the fiber (V_2).

The tribological tests were conducted using a pin on disc tester under the following conditions: unit pressure p = 3 MPa, sliding velocity v = 0.5 m/s, sliding distance s = 5000 m, lubricated with semi synthetic engine oil 10W-40.

Friction contact is shown in Fig. 1. The sample was the cast iron pin and the counter sample the composite disc. Friction force was recorded by measuring device Spider 8 with the inaccuracy of 3% of the measured value. The study was performed on three sets of samples. Samples and counter-sample after tribological tests were tested on a scanning electron microscope.

Fig. 1. Pin on disc contact used in tribological test (pin GJS-400, disc AlMC)

Profilometry test was performed using an optical profilometer with a resolution of 0.01 nm on the vertical axis. The use of mechanical profilometer with a diamond-tipped lead to plastic deformation of the matrix material in the composite and the large spalling of graphite precipitates in the cast iron, which distorts the measurement results [16].

3. Experimental results

3.1. Stereological parameters

Microstructures of the tested composite, showing the extreme positions of the fibers are presented in Figure 2. In Figure 2a predominate fibers arranged vertically (circles and ellipses in the cross-section) of polished cros-section surface

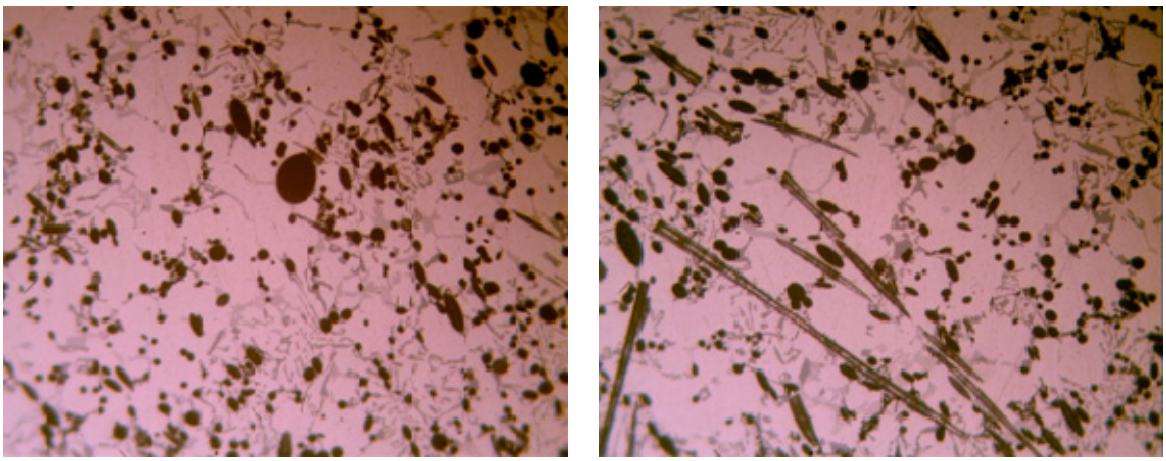

a) b)

Fig. 2. Polished cross section of AC-4700+10%A_F composite used for determining of stereological parameters of alumina fibers: a) fibers placed perpendicularly, b) fibers placed in parallel

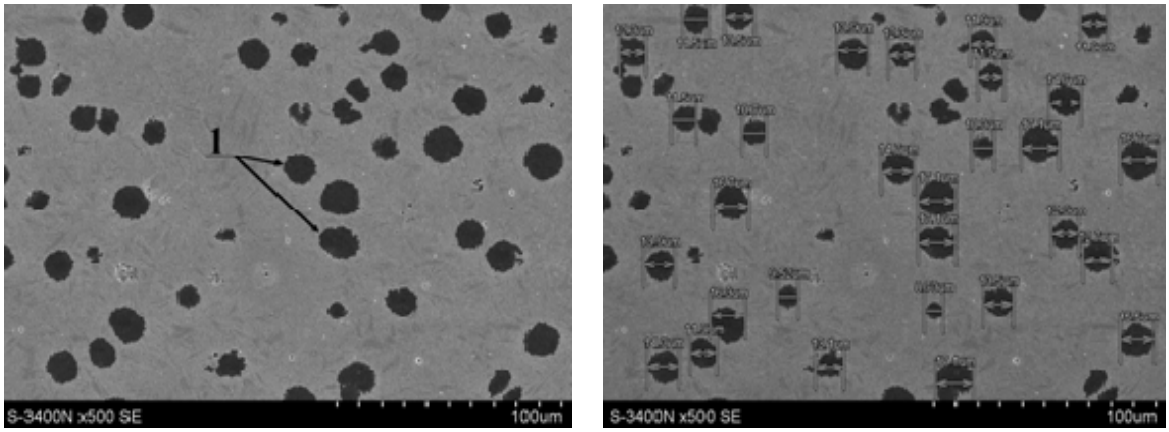

a) b)

Fig. 3. Polished cross sections of EN-GJS-400 cast iron used for quantification of stereological parameters: a) view, 1 – graphite precipitate, b) graphite with diameter measurement, 2 – pearlitic matrix

and the friction surface in contact. In Figure 2b a lot of fibers arranged parallel to the surface of polished cros-section and friction area. The microstructure of tested cast iron and the method of measuring the diameter of graphite precipitates are shown in Figure 3. A histogram of graphite precipitations diameters of cast iron is shown in Figure 4 and Table 1.

3.2. Parameters of 3D model

Using stereological features of graphite precipitations in cast iron and fibers in the composite was built spatial model of the tested contact for three cases, i.e.:

– whole sphere of graphite entering in contact with the composite (sphere),
– sphere worn in 40% (0.6 sphere),
– sphere worn in 70% (0.3 sphere).

The view of contact model is shown in Figure 5 and the position of the spheres in relation to the fibers after removal of

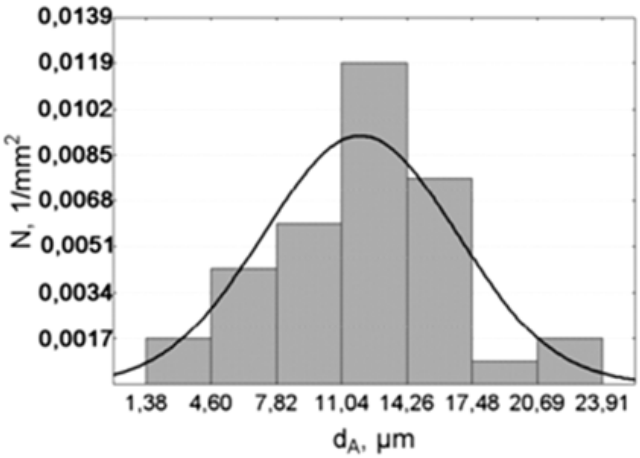

Fig. 4. Histogram of average diameter of graphite precipitations (d_A)

pearlitic cast iron matrix in Figure 6. The symbol V_1 indicates a parallel direction of movement of the pin relative to the position of the fibers and V_2 perpendicular direction.

TABLE 1

Quantitative results of graphite precipitations in spheroidal cast iron

Parameter		Results	σ
Surface fraction of the graphite	%	10,89	0,41
Number of graphite per unit area, N	$1/mm^2$	1216	52
Average area of the particles of graphite, A_A	μm^2	158,50	7,35
Maximum diameter of the particles of graphite, d_{max}	μm	13,24	0,62
Minimum diameter of the particles of graphite, d_{min}	μm	10,56	0,45
Average diameter of the particles of graphite, d_s	μm	11,90	0,49
Elongation ratio of graphite, K	—	1,33	0,05
Maximum distance betweene the pracipitates of graphite	μm	34,65	1,73
Average distance between the grapgite	μm	19,50	0,97
Minimum distance betweene the pracipitates of graphite	μm	4,36	0,21
Index shape of graphite, s	—	0,87	0,04

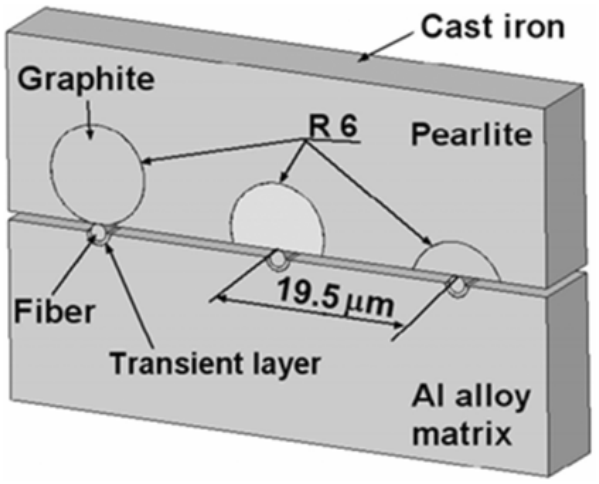

Fig. 5. Graphite and alumina fiber location to sliding surface and stereological parameters of

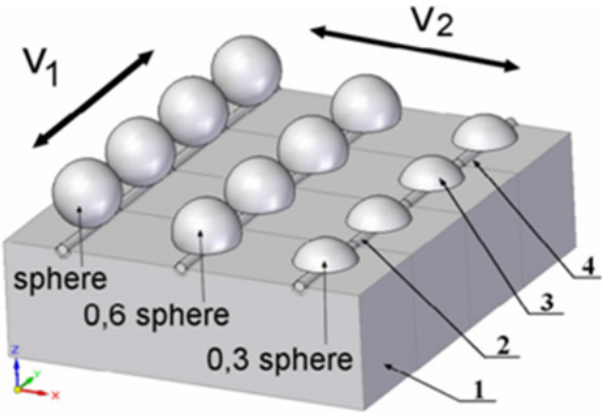

Fig. 6. Solid model of EN-GJS-400/AC-47000 + 10% Al_2O_3F contact with fibers parallel (V_1) and perpendicular (V_2) movement to the friction direction: 1 – matrix, 2 – fiber; 3 – grapfite, 4 – transient layer

3.3. Tribological test

During tribological tests was friction forces measured and recorded. The example of the friction coefficient in dependence on the friction distance is shown in Figure 7.

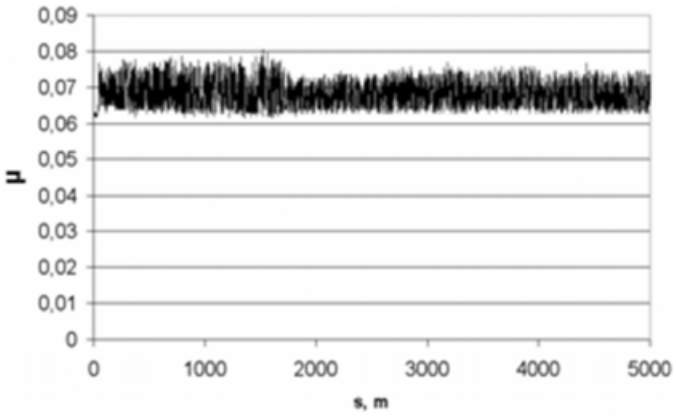

Fig. 7. Coefficient of friction (μ) vs. sliding distance (s) for sliding contact GJS-400/AC-47000 + 10%Al2O3F (p = 3 MPa, v = 0,5 m/s)

3.4. FEM analysis

Distributions of local stresses around of graphite precipitation in the cast iron, and fibers in the composite are shown in Figure 8 and the strains in Figure 9. To facilitate the use of stresses and strains distribution, using software, were determined their maximum values in graphite precipitation and in the matrix of the composite, the boundary layer between the fiber and the matrix and in fibers. These values are summarized in Table 2.

3.5. Microscopic examination

The samples and counter-samples surfaces after friction were observed by scanning microscopy. Selected results are shown in Figures 10-13.

In Figure 11 will be presented the analysis results of chemical composition of piston ring-cylinder liner contact wear products selected from oil by washing with solvent and filtration on a cotton filter. Figure 11a shows a fragment of the fiber Al_2O_3 (peaks of Al and O in Figure 11c), and Fig. 11b piece of graphite (peak C in Fig. 11d).

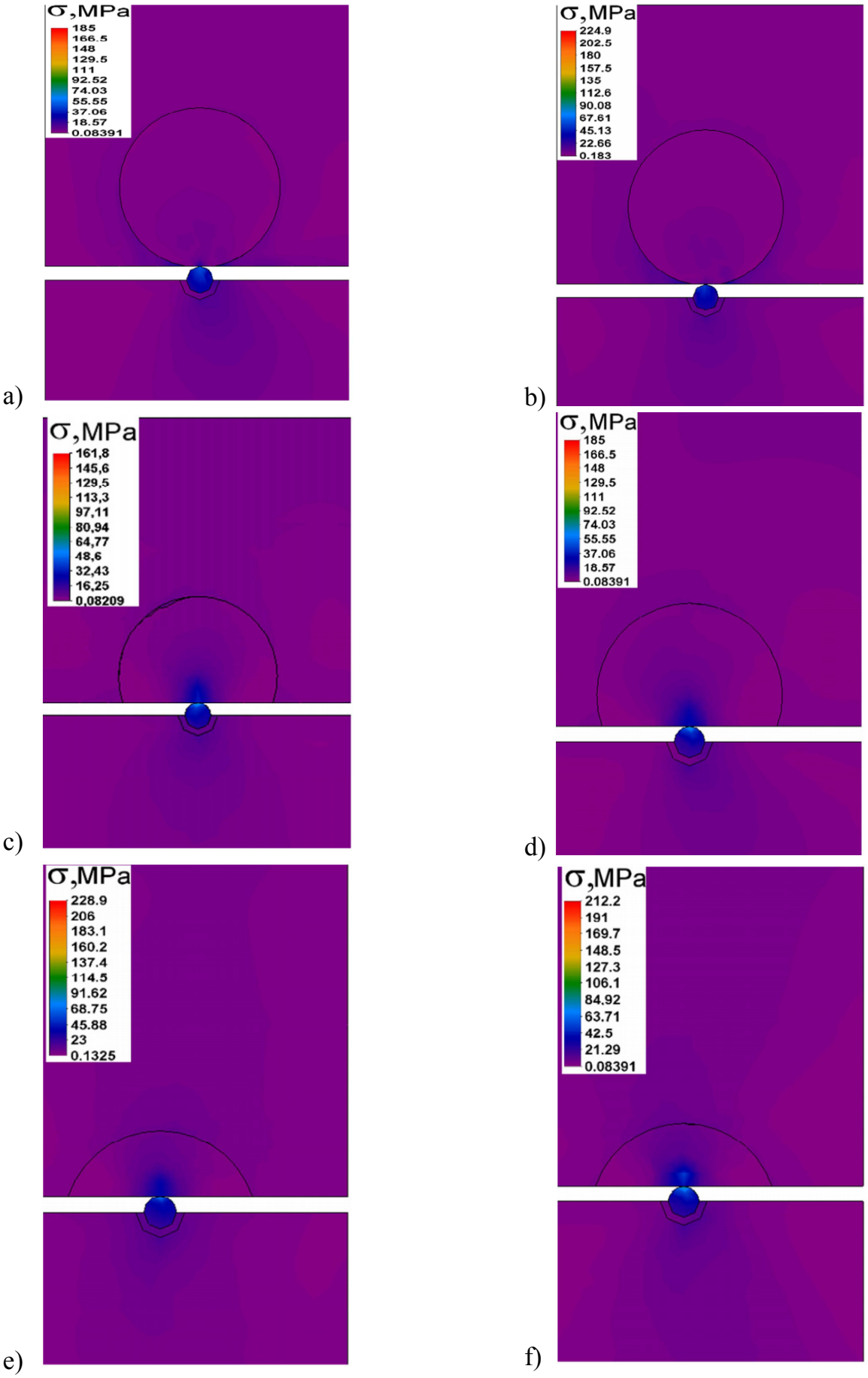

Fig. 8. Distribution of the local stresses in the contact area graphite-fiber Al_2O_3 in the motion of the pin to ⊥ sliding perpendicular to Al_2O_3 fibers (a,c,e) and sliding ─ along to Al_2O_3 fibers (b,d,f)

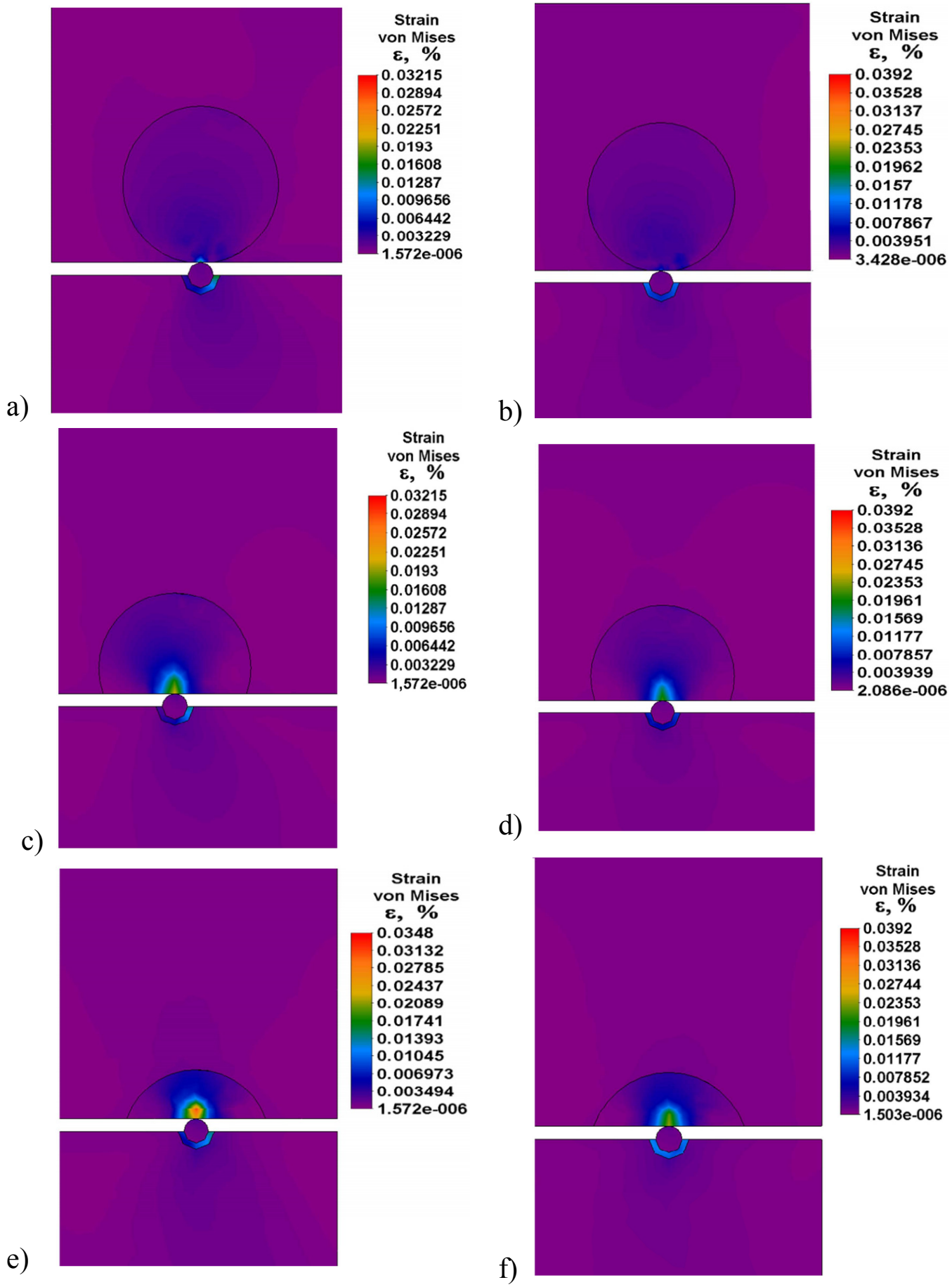

Fig. 9. Distribution of the local strains in the contact area graphite-fiber Al_2O_3 in the motion of the pin to ⊥ sliding perpendicular to Al_2O_3 fibers (a,c,e) and sliding ─ along to Al_2O_3 fibers (b,d,f)

TABLE 2

Statement of the results by means of FEM

	Graphite Precipitate – sphere				Graphite Precipitate – 0.6 sphere				Graphite Precipitate – 0.3 sphere			
	σ (MPa)		ε (‰)		σ (MPa)		ε (‰)		σ (MPa)		ε (‰)	
	─	⊥	─	⊥	─	⊥	─	⊥	─	⊥	─	⊥
Matrix	60.2	27.9	0.011	0.0052	62.5	38.2	0.011	0.007	63.4	39.9	0.011	0.0074
Transient layer	31.9	25.8	0.032	0.026	28.1	28.9	0.028	0.029	31.3	30.9	0.031	0.031
Fiber	142.8	97.3	0.0047	0.0035	197.1	155.3	0.0065	0.005	227.7	212.8	0.0075	0.0069
Pearlite	224.9	184.8	0.025	0.020	204.7	151.1	0.023	0.017	228.8	202.8	0.025	0.023
Graphite	65.1	56.7	0.039	0.034	48.1	42.3	0.029	0.025	59.8	58.1	0.036	0.035

⊥ sliding perpendicular to Al_2O_3 fibers; ─ sliding along to Al_2O_3 fibers.

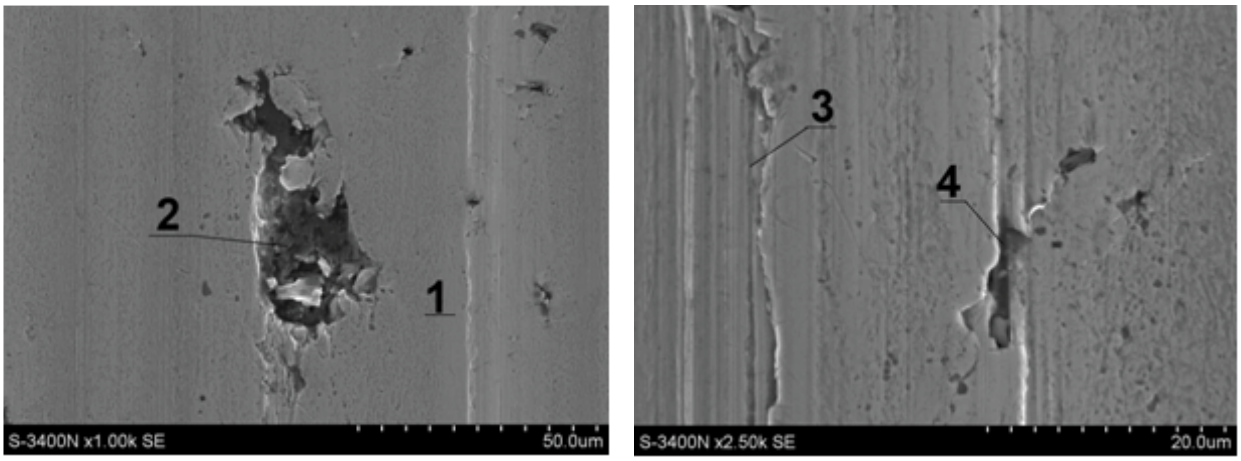

a) b)

Fig. 10. Surface friction of spheroidal cast iron with visible recess after crushed graphite (a) and the release of graphite (b): 1 – areas polished by abrasive wear, 2 – places after crushed graphite, 3 – area of grooves, 4 – plastic deformed matrix covering the place after crushed graphite

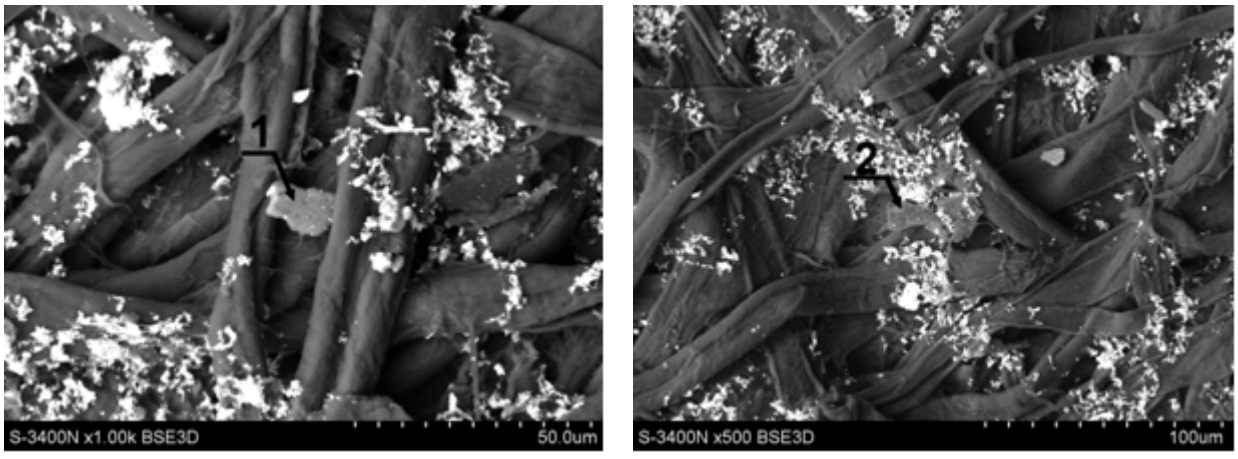

a) b)

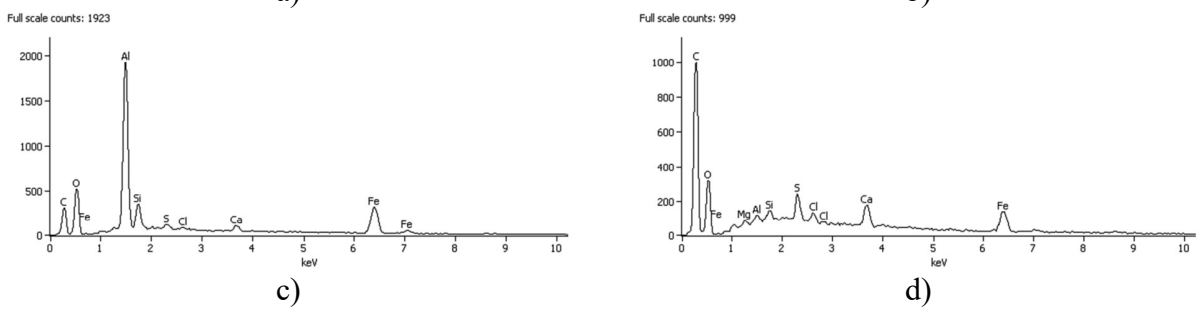

c) d)

Fig. 11. The presence of Al_2O_3 fiber wear debris and chemical analysis (a, c) also graphite wear debris and chemical analysis (b, d) in the oil during rubbing

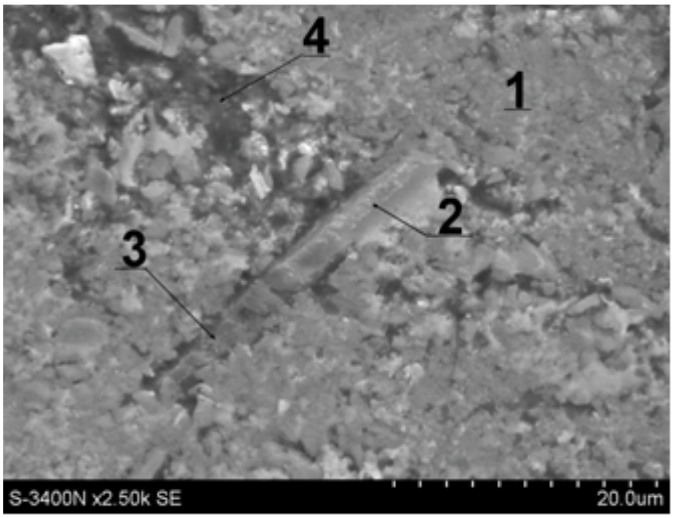

Fig. 12. The fiber of the reinforcing phase in one part broken and in the other protruding from the surface: 1 – matrix, 2 – fiber partially worn, 3 – fiber incrusted in matrix, 4 – valley in matrix action as oil depot

3.6. Profilometric examination

The profilometry test results i.e. 2D and 3D roughness profiles of the composite surface before and after the sliding are shown in Figure 14 and 15.

In the profilometry studies was measured the height at which the fiber Al_2O_3 extends of the matrix material (AC-47000). The average value was 0.2 µm.

4. Discusion of the results

Illustrated in Figure 2 composite surfaces confirm the validity of the adopted extreme positions of fibers, i.e. parallel and perpendicular to the friction surface. Number of parallel fibers does not exceed 10%. Pictures in the Fig. 3 show that the graphite precipitations are almost uniformly distributed in the surface contact with the composite. The average distance between the

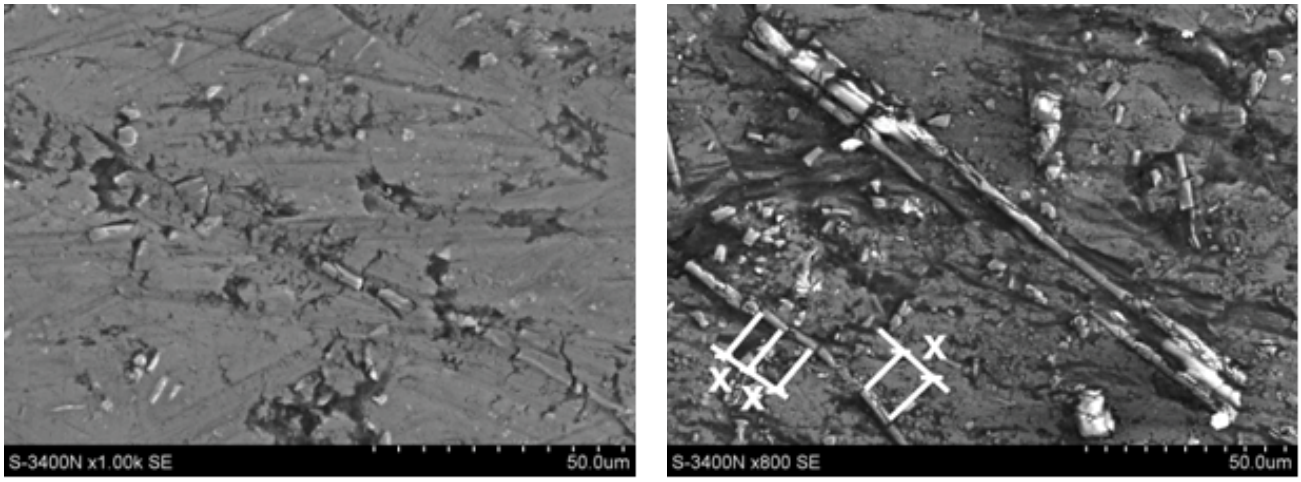

a) b)

Fig. 13. Exposed friction surface of the composite with crushed Al_2O_3 fibers: a) without friction, b) after rubbing: x – crushed fiber section Al_2O_3

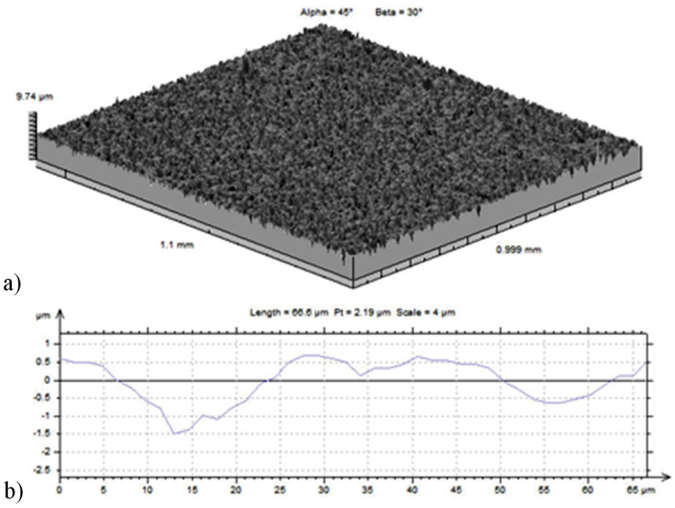

Fig. 14. Profile 3D (a) and 2D (b) composite roughness before rubbing

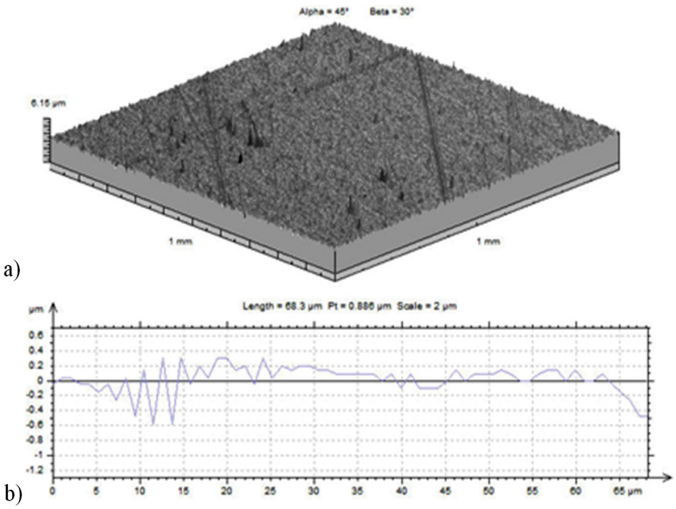

Fig. 15. Profile 3D (a) and 2D (b) composite roughness after rubbing

graphite precipitates of 19.5 μm and a mean fiber diameter of 2 μm confirmed that during sliding of cast iron against composite comes to the local contact of the hard fiber with a hard pearlitic matrix (on the average length of 19.5 μm), which can influence mitigation of friction. From Figure 4 it follows that the amount of graphite precipitates with a large diameter d > 20 μm is low, which prevents formation of large craters after spalling of graphite. Shown in Figures 5 and 6 models of graphite spheres with the fibers contacts show that it is possible to micro bending of fibers at the time of contact with the worn sphere (0.6 and 0.3 sphere) if under fibers are hard precipitation of silicon inhibiting strains of the matrix. Oscillations of friction coefficient (Fig. 7) between 0.062 and 0.074 may indicate a local taking of pearlitic cast iron matrix with a solution of silicon in aluminum (a) w in the composite matrix.

Comparing the levels of friction coefficient in contact grey cast iron/composite (μ = 0.1 [13]) and in contact nodular cast iron/composite (μ = 0.07) it can be stated, the shape of graphite causes a reduction of friction. The graphite spheres in GJS-350 undergo wear quickly as the flakes in GJL-250 cast iron. More graphite debris in oil between the contact surfaces reduced friction. The average distance between graphite lamellas is smaller than the one between spheres. This may be a second reason for oscillations of friction forces in contact with nodular cast iron. In the praxis will it result in higher vibrations of an engine with nodular cast iron piston rings.

Based on the Figures 7 and 8 and Table 2, it can be concluded that the area of maximal effort in graphite are located at a depth of approx. 2 μm. In the getting into the contact zone precipitate of graphite (sphere, Fig. 8), the largest stresses are located at the sphere contact point with fiber and at the edges of the matrix. This may results in spalling of soft graphite. The sharp edge of matrix will try to turn the Al_2O_3 fiber around the axis leading to the loosening and uprooting from the matrix. The second consequence of this phenomenon is the indentation of Al_2O_3 fibers in a soft composite matrix. This is clear evidenced by photographs taken on the SEM microscope (Fig. 13).

Observation by SEM of the composite surface after rubbing, allows to recognize wear mechanism (Fig. 12). The smoothing of the area (1) is the result of wear of the taking of and probably the rolling of Al_2O_3 fibers fragments. From the matrix protrudes laterally cracked piece of fiber (2) with visible traces of abrasive wear (fine scratches). Part of this fiber (3) is recessed in the matrix. Next to the fiber arose cavities demonstrating the loosening of the intermediate layer of the fiber caused by friction forces, seeking to turn the fiber. This is confirmed by profilometry studies (oscillations in the left side of the 2D-graph, Fig. 15b). On the surface of the composite matrix are shown valleys (4) in which can be accumulated oil reducing friction and wear How do the oil contained between the fibres and cast iron acts on the contacting surfaces, will be shown in Figure 16.

Like it appears from microscopic examinations of oil taken from the contact after friction, were found in it the presence of graphite and of Al_2O_3 fibers wear products (Fig. 11). The presence of graphite in oil allowed obtaining a low coefficient of friction (Fig. 7).

Microreservoir of oil closed by the fibers protruding from a matrix of the composite are locally being formed. Extreme positioning of perlite plates (parallel and perpendicular to the friction surface) presented in Figure 16 shows that it may occur the creation of hydrodynamic effects and slight elevation of one material relative to the other causes a decrease in stresses and local strains as well as friction forces.

On the micrograph in Figure 10a can be seen the surface of the ferrite, being a component of the pearlite, plastically deformed during rubbing against Al_2O_3 fibers.

The stresses occurring in the matrix of the composite, while the friction along the fibers are two times greater than the friction transverse to the direction of the Al_2O_3 fibers. This may be due to the average distance between the fibers providing the dispersion of Al_2O_3. The values of stresses and strains in the intermediate layer are small and irrelevant, regardless of the direction of friction.

The values of stresses and strains in the fibers of Al_2O_3 increase with progressive wear of graphite spheres (from sphere

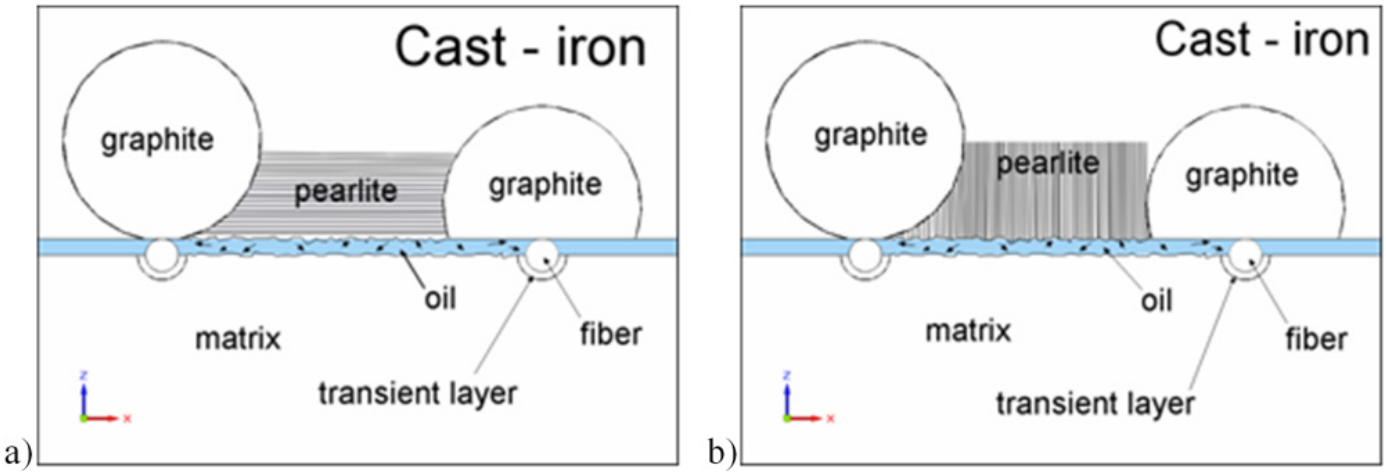

Fig. 16. The effect of the lubricating medium in the oil reservoir formed between the Al2O3 fibers and cast iron pressure against the composite when the perlite plates arranged in parallel (a) and perpendicular (b) to the friction force

to sphere 0.3). This is because of a lower fraction of graphite, which take over the deformations.

The value of stresses in graphite is significant, reaching 65 MPa, what leads to its wear and spalling from the friction surface.

5. Conclusions

Based on the analyze of the results of study following conclusions are possible:

1. Performance of stereological tests of nodular cast iron and a composite with fibers enables the construction of a spatial model of contact and make the calculations of local distribution of stresses and strains in the vicinity of graphite precipitates and fibers.
2. Calculated by using FEM local values of stresses and strains as well as microscopic and profilometric examinations show the most strained places in materials of rubbing parts, which help to explain the wear mechanisms of GJS-400/AC-47000 + 10% Al_2O_{3F} contact.
3. The main wear mechanisms in nodular cast iron piston ring-AlMC cylinder liner contact are abrasive wear of alumina fibers by paerlitic matrix of cast iron and taking between pearlite and composite matrix.
4. Taking between cast iron pearlitic matrix and composite matrix (Si soloution in Al) can lead to oscillations of friction forces.

REFERENCES

[1] R.M. Lazzarin, M. Noro, An experience in Italy Applied Thermal Engineering **90**, 509-520 (2015).
[2] B. Bhushan, B.K. Gupta, Handbook of Tribology, USA, (1991).
[3] K. Hirasata, K Hayashi, Y Inamoto, Wear **263**, 790-800 (2007).
[4] D.G. McCartney, A.V. Wills, Appl. Math. Modelling **12** (8), 125-132 (1998).
[5] Ch. Chengxi LEIa, J. Cuib, Z. Xinga, H. Fua, H. Zhaoa, Physics Procedia **25**, 118-124 (2012).
[6] A. Malakizadia, I. Sadikb, L. Nyborga, Procedia CIRP **8**, 188-193 (2013).
[7] B.K. Prasad, Materials Science and Engineering **456**, 373-385 (2007).
[8] S. Wang, D. Daloz, F. Bruneseaux, G. Lesoult, Materials Science and Engineering **27**, 1-6 (2011).
[9] A. Wang, H. Chengb, J. Lib, Ruijie Procedia Engineering **31**, 360-365 (2012).
[10] N. Bonora, A. Ruggiero, International Journal of Solids and Structures **42**, 1401-1424 (2005).
[11] Y. Ma, SAE Technical Paper 1205 (2013).
[12] T. Węgrzyn, J. Piwnik, Ł. Wszołek, W. Tarasiuk, Archives of Metallurgy and Materials **60** (4), 2625-2630 (2015).
[13] A. Posmyk, H. Bakowski, Tribology Transactions **56** (5), 806-815 (2013).
[14] A. Posmyk, H. Bakowski, Composites **9** (1), 29-33 (2009).
[15] M. Tkayaa, S. Mezlinic, M. Mansoria, H. Zahouanib, Wear **267**, 535-539 (2009).
[16] A. Posmyk, P. Chmielik, Composites **10** (3), 229-234 (2010).